Computers in Biology and Medicine 175 (2024) 108488

Contents lists available at ScienceDirect

Computers in Biology and Medicine

journal homepage: www.elsevier.com/locate/compbiomed

The role of the extracellular matrix in the reduction of lateral force transmission in muscle bundles: A finite element analysis

Silvia Spadoni [a], Silvia Todros [a,*], Carlo Reggiani [b], Lorenzo Marcucci [b,1], Piero G. Pavan [a,c,1]

[a] Department of Industrial Engineering, University of Padova, Padova, Italy
[b] Department of Biomedical Sciences, University of Padova, Padova, Italy
[c] Fondazione Istituto di Ricerca Pediatrica Città Della Speranza, Padova, Italy

ARTICLE INFO

Keywords:
Muscle bundle
Aging
Lateral force transmission
Extracellular matrix
Finite element method

ABSTRACT

Background and objective: Aging is associated with a reduction in muscle performance, but muscle weakness is characterized by a much greater loss of force loss compared to mass loss. The aim of this work is to assess the contribution of the extracellular matrix (ECM) to the lateral transmission of force in humans and the loss of transmitted force due to age-related modifications.

Methods: Finite element models of muscle bundles are developed for young and elderly human subjects, by considering a few fibers connected through an ECM layer. Bundles of young and elderly subjects are assumed to differ in terms of ECM thickness, as observed experimentally. A three-element-based Hill model is adopted to describe the active behavior of muscle fibers, while the ECM is modeled assuming an isotropic hyperelastic neo-Hookean constitutive formulation. Numerical analyses are carried out by mimicking, at the scale of a bundle, two experimental protocols from the literature.

Results: When comparing numerical results obtained for bundles of young and elderly subjects, a greater reduction in the total transmitted force is observed in the latter. The loss of transmitted force is 22 % for the elderly subjects, while it is limited to 7.5 % for the young subjects. The result for the elderly subjects is in line with literature studies on animal models, showing a reduction in the range of 20–34 %. This can be explained by an alteration in the mechanism of lateral force transmission due to the lower shear stiffness of the ECM in elderly subjects, related to its higher thickness.

Conclusions: Computational modeling allows to evaluate at the bundle level how the age-related increase of the ECM amount between fibers affects the lateral transmission of force. The results suggest that the observed increase in ECM thickness in aging alone can explain the reduction of the total transmitted force, due to the impaired lateral transmission of force of each fiber.

1. Introduction

Independence in daily life activities in the elderly is strongly limited by age-related loss of muscle strength and Reduced Joint Mobility (RJM) [1]. Furthermore, in addition to the impact on quality of life, RJM is also associated with an increased risk of falls and hospitalization [2], with a consequent impact on social costs. Functional impairment [3,4] and loss of independence [5] have a direct relationship with one of the main causes of RJM, muscle weakness [6], which is recognized as an independent factor of risk in the mortality of elderly people [1,7–10]. Therefore, it is of crucial importance to understand the reasons behind age-related decline in muscle function.

Interestingly, muscle weakness is characterized by a disproportionate loss of force compared to the loss of muscle mass. In fact, the decrease in muscle mass with aging (sarcopenia) is accompanied by a much more rapid decrease in muscle strength (dynamopenia) [11]. However, the causes of this imbalance are mostly unknown and may involve alterations in muscle architecture and tendon stiffness, reduced neural drive, motoneuron, and neuromuscular junction damage, loss of motor units, impaired excitation-contraction coupling, reduced myosin density associated with a decrease in fiber specific tension [12].

Another possible reason for the disproportionate loss of force during

* Corresponding author. Department of Industrial Engineering, University of Padova, via Venezia 1, 35131, Padova, Italy.
E-mail address: silvia.todros@unipd.it (S. Todros).
[1] Co-last authors.

https://doi.org/10.1016/j.compbiomed.2024.108488
Received 8 January 2024; Received in revised form 28 March 2024; Accepted 15 April 2024
Available online 17 April 2024

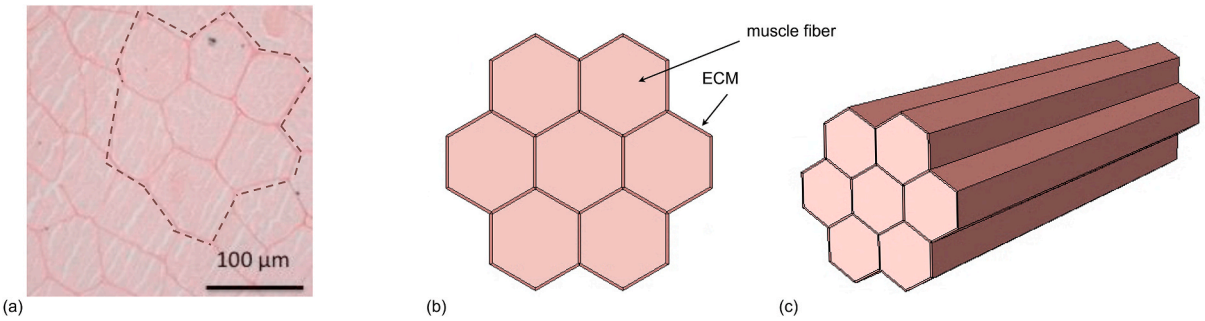

Fig. 1. Transverse section of a histological sample of human muscle vastus lateralis [38] where a muscle bundle is outlined with a dashed line (a); transverse section (b) and 3D view (c) of the simplified geometry of a muscle bundle composed of fibers (pink) and ECM (brown).

aging is an impairment in force transmission mechanisms. The contractile forces generated from each muscle fiber are added up at the bundle level and transmitted to the tendons to generate the motion of the skeleton. Force transmission is ensured both longitudinally and laterally. The longitudinal transmission of the force occurs along the main axis of the muscle fibers, while the lateral transmission of force is achieved transversally to the fiber axis. The latter mechanism involves the extracellular matrix (ECM), as experimentally shown in frogs [13], rats [14,15], and mice [16]. A modification of the capability of lateral force transmission through the ECM has been proposed to play a key role in the above-mentioned loss of transmitted force [14,17].

The ECM plays a key role in the macrostructural arrangement of the muscle, setting the fibers in bundles, the bundles in fascicles, and integrating them with the aponeurosis and the tendons. The ECM can be roughly divided into three hierarchical substructures, i.e., endomysium, perimysium, and epimysium [18]. The endomysium is a highly ordered mesh-like network formed mainly by an equal amount of type I and III collagen, which runs around single muscle fibers and shows a nonlinear stress-strain relationship with increased sarcomere length. The perimysium surrounds bundles of muscular cells and has a different structure and composition, being primarily formed by type I collagen. Thus, this composition is similar to that of the tendon, which also shows some continuity with the perimysium. Finally, the epimysium surrounds the entire muscle and allows it to contract while maintaining its structural integrity.

During human aging, a relevant modification has been found in the morphological and structural characteristics of muscle bundles [19,20]. In detail, increased ECM thickness, accompanied by increased collagen concentration, modification in elastic fiber density, and increased fat infiltration of skeletal muscle, has been observed [19]. Moreover, biochemical alterations, such as decreased collagen turnover followed by accumulation of enzymatically mediated collagen crosslinks, have been reported [20]. Among these age-related modifications, particular attention is focused on the increase of the ECM content in muscle bundles, due to the potential effects on the muscle efficiency in force transmission.

However, quantitative knowledge of the role of the ECM in muscle weakness in elderly humans is still lacking. The difficulties in obtaining quantitative data on human samples led to the almost exclusive presence in the literature of data on other mammals. Therefore, the Finite Element Method (FEM) can be useful to infer this information in human subjects in a non-invasive way. Computational modeling can replicate the behavior of biological systems based on known properties of the system components [21–24], described using suitable mathematical models [25,26], and can serve as an important complement to human experimental studies, providing additional knowledge even in the absence of experimental samples. For this purpose, in this work, the role of the ECM in the loss of laterally transmitted force in aging is estimated at the mesoscopic level. In particular, the increase of the fraction of the cross-sectional area (CSA) occupied by ECM – due to parallel muscle fiber atrophy and ECM thickening – is considered, as observed in humans [27] and rodents [17].

Several micromechanical and multiscale models have been adopted to study the contribution of ECM to force transmission. Yucesoy et al. [28,29] developed a FEM fiber-matrix model based on two single layers: a muscle fiber layer and an ECM layer, which were elastically linked to account for the *trans*-sarcolemma attachments of the fiber cytoskeleton and ECM. With this approach, they evaluated the lateral transmission of force, even though the geometry of the model was not fully representative of the physiological structure of the muscles. Zhang et al. [30] developed a 2D FEM model of a single muscle fiber, highlighting that most of the generated force is transmitted to the end of the myofiber through shear to the endomysium. In a further development of this model [31], the contribution of transmembrane proteins between fiber and ECM was also considered, showing that force transmission and stress distribution are not affected by the tensile stiffness of transmembrane proteins. However, muscle fibers with insufficient transmembrane proteins near their ends were found to transmit a reduced force compared to the case with more proteins.

More generally, several FEM models have shown how muscle force transmission is influenced by passive mechanical properties [32]. Micromechanical models based on repeating unit cells reconstructed from histological cross-sections of rabbit muscles were developed to study the effects of fiber and fascicle microstructure on the macroscopic shear modulus under normal and disease conditions [33,34]. Zhang et al. [35] developed a FEM model of muscle bundles based on a honeycomb-shaped structure, designed by means of a pixel-based reproducing kernel particle method, which allows for a smooth transition in material properties at interfaces. The force generated by three muscle types (young, adult, and old) was predicted for isometric, concentric, and eccentric contractions. They demonstrated that an age-related increase in the stiffness and thickness of passive tissue reduces the force generation capability under concentric contraction, while maintaining the force generation capability under eccentric contraction.

Unlike most studies in the literature, the present work is strictly based on experimental data taken from human musculoskeletal fibers and bundles [36–38]. The intrinsic and extrinsic properties of the ECM, i.e., tensile stiffness and relative amount in the CSA, have been characterized in young and elderly human bundles, imposing stepwise elongation in passive condition and estimating the separated contribution to passive tension given by inter- and intra-filament structures. These data confirm the predominant role of the ECM in generating passive tension when a bundle is stretched and show that the total passive tension is higher in the bundles of elderly subjects compared to young subjects. Interestingly, these results suggest that the higher passive tension can be fully explained by the higher amount of ECM in the CSA of the bundles of elderly subjects and not by an age-related modification of the tensile stiffness of the ECM.

Prompted by the experimental evidence, a FEM approach is used to

evaluate the sole effect of increasing the amount of ECM between fibers due to aging on the lateral transmission of force at the bundle level. FEM models of human muscle bundles are developed for young and elderly subjects, considering fibers connected through an ECM layer of different thickness. Specific constitutive models are adopted to describe both the active and passive behavior of muscle fibers and the mechanical response of the ECM. Constitutive parameters are based on experimental data obtained in previous studies [38] at the fiber and bundle level in human biopsies, performed in young and elderly subjects. The numerical analyses proposed are inspired by experimental protocols applied to rat muscles, reproducing them on the scale of human bundles.

2. Methods

2.1. Development of FEM models of muscle bundles

The models are created with ABAQUS CAE (SIMULIA™, Dassault Systèmes, France). Two FEM models of a typical human bundle are constructed, one for a young subject and one for an elderly subject, both composed of seven fibers and the surrounding endomysium (Fig. 1). These models will be indicated in the following as the young bundle and the elderly bundle, respectively.

Starting from a histological section of a sample of human muscle vastus lateralis [38], the geometry is simplified, assuming a regular hexagonal cross section for the fibers and differentiating the young and elderly bundles based on the thickness of endomysium. According to previously reported experimental data, the average CSA of the muscle fibers is assumed to be 7669 μm^2, both for young and old subjects, while the CSA of endomysium results of 1853 μm^2 and 4779 μm^2 for young and elderly bundles, respectively. The average value of the ECM thickness around each muscle fiber (dark brown regions in Fig. 1 b and c) is 0.97 μm and 2.80 μm for young and elderly bundles, respectively. The length of the bundle (1000 μm) is the same for the two models. Each single fiber has a hexagonal transversal section, corresponding to an equivalent diameter of 99.0 μm. The transversal section of the bundles corresponds to an equivalent diameter of 266.7 μm and 272.8 μm for the young bundle and the elderly bundle, respectively. The equivalent diameter is calculated as $(4\ A/\pi)^{1/2}$, being A the area of the transversal section.

The contact conditions applied in the FEM models between the regions corresponding to fibers and ECM are defined assuming a perfect bounding. The use of multi-point constraints makes it possible to impose the boundary conditions to fibers and endomysium as explained below.

The fiber and ECM regions are discretized with 8-node hexahedral elements of hybrid type (pressure-displacement). This ensures the almost-incompressibility behavior described by the constitutive models defined in the following sections, without introducing volume strain locking and numerical instabilities in the solution. The average length of elements is 16 μm for the muscle fiber regions and 0.5–0.9 μm for the ECM regions, along the direction of the ECM thickness. The bundle model of young subjects has about 22,000 elements and 121,500 degrees of freedom, while the bundle model of elderly subjects has about 81,000 elements and 394,000 degrees of freedom.

Table 1
Constitutive parameters for skeletal muscle fibers.

Parameter	Value	Description
A (MPa)	1.6	parameter related to the passive tensile stiffness of the fiber according to Equation (1)
P_0 (MPa)	0.4	maximum isometric stress in Equation (2)
S (s^{-1})	6.0	parameter that regulates the activation rate in Equation (3)
λ_{min}	0.491	minimum stretch of the force-length function described by Equation (4)
λ_{opt}	0.904	optimum stretch of the force-length function described by Equation (4)
K_c	5.0	scalar parameter in the force-velocity function defined by Equation (5)
$\dot{\lambda}_{max}$	−1.94	maximum value of stretch rate in the force-velocity function defined by Equation (5)
α_1 (kPa)	0.821	parameters of the strain energy function in Equation (7)
α_2	1.79	
K (kPa)	10^4	

2.2. Constitutive modeling of muscular fibers and endomysium ECM

The constitutive model of muscular fibers is characterized by local transversal isotropy, being the plane of isotropy perpendicular to the spatial direction of the muscle fibers. The effects of sarcomere elements and connective components are considered through homogenization at the level of each single finite element volume. The constitutive model assumed to describe the mechanical response of muscle fibers and its relevant functions were tested in previous works [27,39–41], in comparison with both literature and original experimental data. The constitutive model showed to properly simulate the mechanical response of muscle fibers in several scenarios of boundary conditions.

Muscle fibers are modeled through a Hill-type three-elements model, where active and passive components are based on human fiber experiments [36]. The stress response of a fiber is supposed to be the sum of a passive P_p and an active P_a term. The passive term is assumed to be:

$$P_p = \begin{cases} 0 & \lambda_f \le 1 \\ A\left(\lambda_f - 1\right)^2 & \lambda_f > 1 \end{cases} \tag{1}$$

where λ_f represents the stretch of the fiber and A is a parameter that has the dimension of stress. The active stress, generated by a fiber contraction is defined as:

$$P_a = P_0 f_a(t) f_l(\lambda_m) f_v(\dot{\lambda}_m) \tag{2}$$

The scalar P_0 is the maximum isometric stress of the fiber; f_a is the activation function, depending on the activation level of the fiber at the current time t; f_l is the force-length function, depending on the sarcomere stretch λ_m; f_v is the force-velocity, depending on the sarcomere stretch rate.

For the activation time range, starting from zero, the activation function is defined by:

$$f_a(t) = 1 - \exp(-S \cdot t) \tag{3}$$

where S is a parameter that regulates the activation rate. The force-length function f_l is assumed as:

$$f_l(\lambda_m) = \begin{cases} \dfrac{\lambda_m - \lambda_{min}}{\lambda_{opt} - \lambda_{min}} \cdot \exp\left[\dfrac{\left(2 - \lambda_{min} - \lambda_m - \lambda_{opt}\right)\left(\lambda_m - \lambda_{opt}\right)}{2\left(\lambda_{min} - \lambda_{opt}\right)^2}\right] & \lambda_m > \lambda_{min} \\ 0 & \lambda_m \le \lambda_{min} \end{cases} \tag{4}$$

where the parameters λ_{min} and λ_{opt} represent the minimum value of the sarcomere stretch in a concentric contraction and its value at the optimal length, respectively. The force-length function accounts for the effects of a change in sarcomere length on the contraction force. Due to the precise geometry of the sarcomere, only a small range of its total length corresponds to the optimal overlap of all pulling molecular motors with the pulled thin filaments. For this reason, the stress generated by a muscle fiber is reduced when its length is far from the optimal length.

Finally, the force-velocity function f_v is defined according to the typical hyperbolic shape:

$$f_v(\dot{\lambda}_m) = \begin{cases} \dfrac{1 - \dot{\lambda}_m / \dot{\lambda}_{max}}{1 + k_c \dot{\lambda}_m / \dot{\lambda}_{max}} & \dot{\lambda}_{max} < \dot{\lambda}_m \le 0 \\ 0 & \dot{\lambda}_m \le \dot{\lambda}_{max} \end{cases} \tag{5}$$

being k_c a scalar parameter, $\dot{\lambda}_m$ the stretch rate of the sarcomere and $\dot{\lambda}_{max}$ its (negative) maximum value for a concentric contraction.

The stress response along the fibers along is then coupled in a 3D

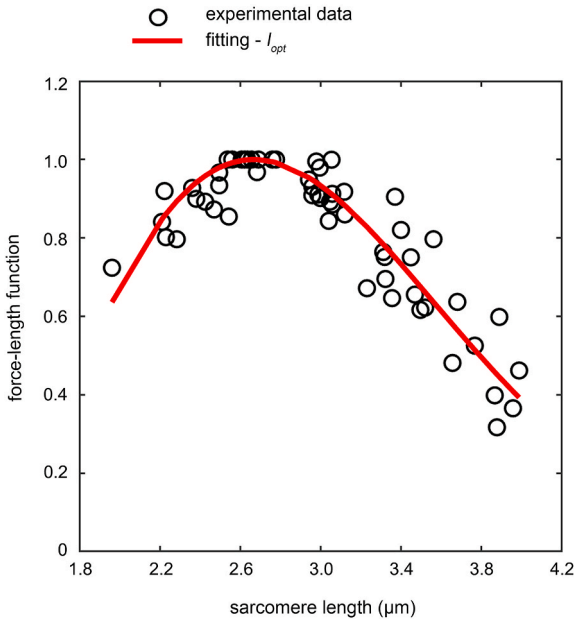

Fig. 2. Fitting of the experimental data acquired by Gollapudi et al. [42] by optimizing the force-length function. The experimental data are normalized by dividing the sarcomere length by the optimal sarcomere length l_{opt}.

constitutive relationship for the first Piola-Kirchhoff stress tensor **P**:

$$\mathbf{P} = \mathbf{P}_{iso} + \left(P_p + P_a\right)\mathbf{F}\cdot(\mathbf{n}_0 \otimes \mathbf{n}_0) \tag{6}$$

where $\mathbf{n}_0$ is the unit vector that defines the spatial orientation of the fiber in the undeformed configuration, **F** is the deformation gradient, and $\mathbf{P}_{iso}$ represents an isotropic term of stress, deduced via a standard derivative from the following strain energy function:

$$W_{iso} = \alpha_1\, exp[\alpha_2(\widetilde{I}_1 - 3)] + \frac{K}{2}(J-1)^2 \tag{7}$$

where J is the Jacobian of the deformation gradient and $\widetilde{I}_1$ the first principal invariant of the isovolumetric part of the right Cauchy-Green strain tensor $\widetilde{\mathbf{C}} = J^{-2/3}\mathbf{F}^T\mathbf{F}$. The scalar K is used as a penalty parameter to ensure almost-incompressibility and, finally, the constitutive parameters α_1 and α_2 are fitted according to the tensile stress-strain response. The set of constitutive parameters for muscle fibers is reported in Table 1. The constitutive parameters of equations ((1), (3), (5) and (7) have been set according to Sharafi et al. [36]. Equation (4) has been fitted to the experimental data of the force-length function for human subjects proposed by Gollapudi et al. [42] and shown in Fig. 2.

The ECM is assumed to be an isotropic and almost-incompressible elastic material. Its tensile response has been characterized in previous works [37,38], showing an almost-linear stress-strain behavior even in a regime of large strains. A neo-Hookean constitutive model, defined by the following strain energy function, is adopted for this tissue:

$$W_{ECM} = \frac{1}{2}K_{ECM}(J-1)^2 + \frac{\mu_{ECM}}{2}(\widetilde{I}_1 - 3) \tag{8}$$

The parameter μ_{ECM} is the initial shear modulus, set to 270 kPa. The same mechanical properties are assumed for the ECM of young and elderly bundles. The constitutive parameter K_{ECM} is the bulk modulus. It is used as a penalty parameter to ensure the almost-incompressibility and is set to 135 MPa, corresponding to a Poisson's ratio of 0.499 at small strains.

2.3. FEM analyses

The effect on lateral force transmission is analyzed by mimicking, at the bundle level, two experimental protocols at the whole muscle level from the literature.

In the first experiment, Huijing et al. [15] showed that the decrease of the total longitudinally transmitted force obtained cutting from one to

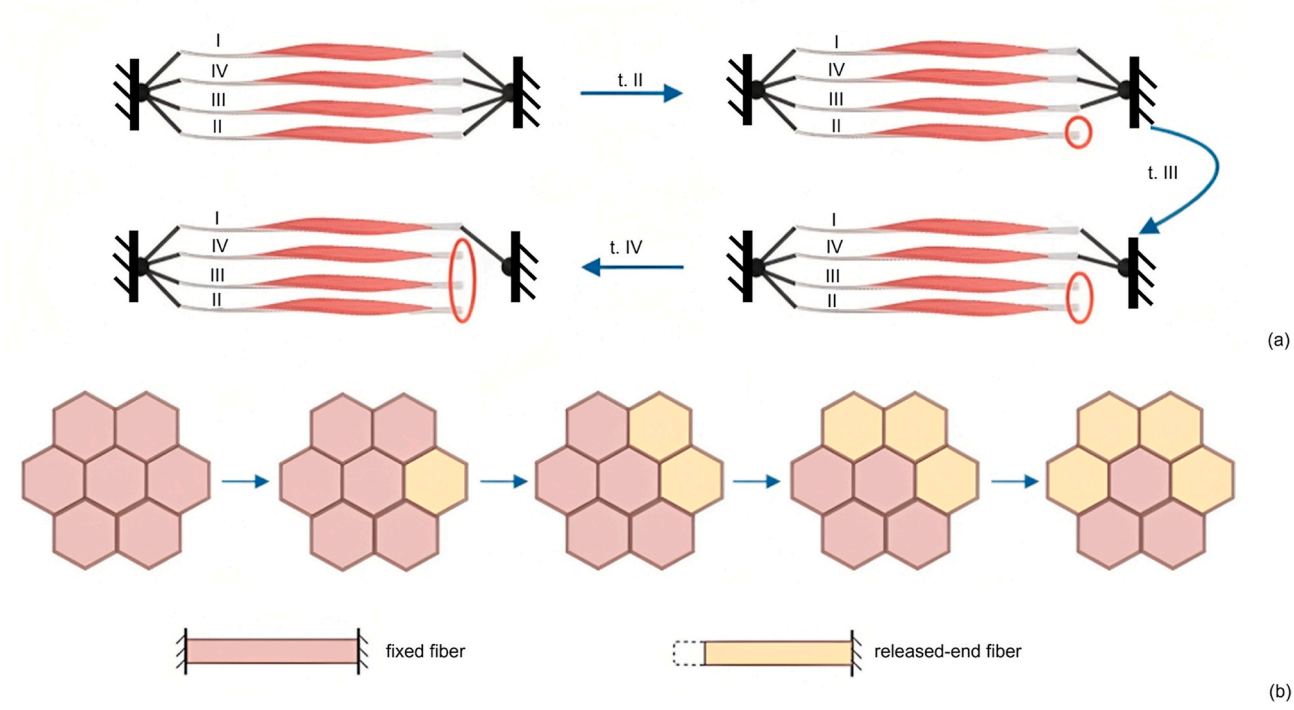

Fig. 3. Scheme of the experimental protocol by Huijing et al. [15], where subsequent tenotomy of tendons II, III and IV are shown (a); schematic description of the numerical simulation carried out on the bundle (b). For fixed fibers, the boundary conditions of the ends are prescribed to impose null displacements along the fiber axis; for released-end fibers, only one end has prescribed null displacements, while the other end is free to move along the fiber axis.

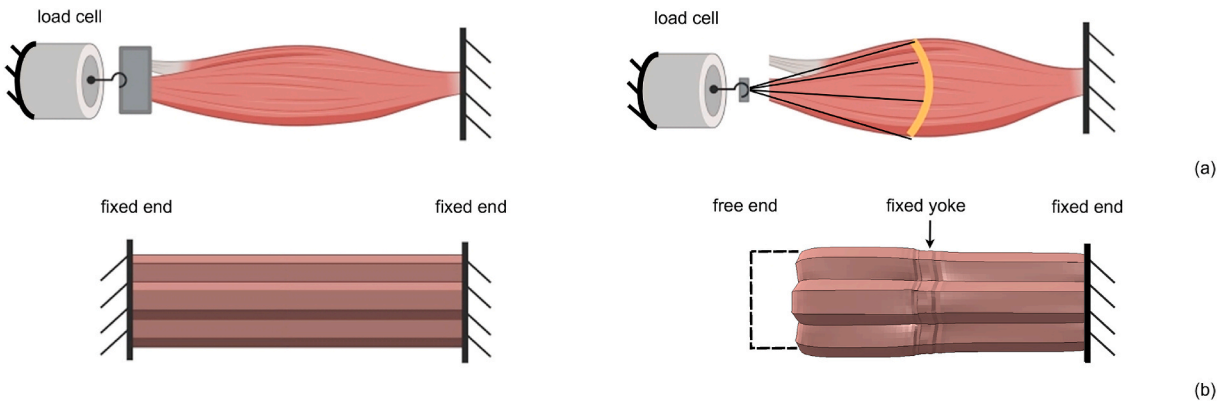

Fig. 4. Scheme of the experimental protocol by Ramaswamy et al. [14], where the isometric state is shown on the left and the contraction with yoke and the free distal head is displayed on the right (a); schematic description of the numerical procedure applied at the bundle level (b). The boundary conditions for the nodes of the fixed ends are prescribed to impose null displacements along the bundle axis. In the middle section of the bundle, where the fixed yoke is placed, the nodes on the lateral surface of the bundle are fixed along the axis bundle.

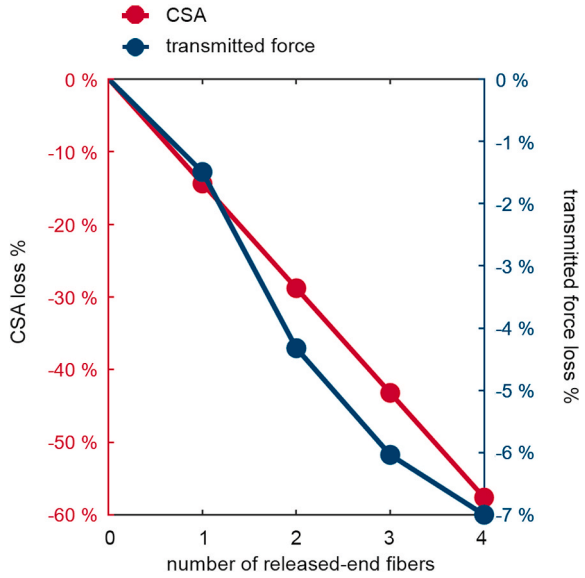

Fig. 5. Percentage loss of muscle CSA and of transmitted force for the young bundle as a function of the number of fibers released. Different scales are adopted for CSA and transmitted force variation. The drop in the total longitudinally transmitted force is one order of magnitude lower than the loss of CSA.

three of the four distal tendons in a rat extensor digitorum longus (EDL) muscle was much lower than the expected value considering the amount of CSA released. These findings suggest the importance of the lateral transmission of force through the ECM. Fig. 3 a shows a schematization of this experimental protocol, while Fig. 3 b describes the analysis carried out in the present work at the bundle level. The fibers are initially in isometric contraction. Subsequently, one to four fibers are progressively released at one end, keeping them always contracted. The transmission of the contraction force is evaluated by considering the amount of reaction force measured at one end of the bundle.

Ramaswamy et al. [14] analyzed the ratio between longitudinal and lateral force transmission in young, old, and very old rats evaluating muscular contraction under different boundary conditions. In the experimental setup shown in Fig. 4, the longitudinal force is the force transmitted in isometric condition, when the tendons are kept fixed, while the lateral force is the force transmitted through a joke applied in the middle section of the EDL muscle when one of its ends is released. By this experimental scheme, it was shown that the ratio of lateral and longitudinal forces decreases with age. This corresponds to an impaired ability to transmit forces laterally in old and very old rats. Here, this protocol is simulated at the bundle level (Fig. 4 b), comparing the results for young and elderly bundles.

A non-linear static algorithm was adopted for all analyses in ABAQUS Standard (SIMULIA™, Dassault Systèmes, France), accounting both for material and geometric non-linearity. The analyses were extended for a total time range of 2 s, to have an almost total recruitment of fiber contraction, according to equation (3). Considering the value assumed for the activation rate (parameter S in Table 1), the activation function f_a assumes a value of 0.998 at the end of the analyses, when numerical results related to the effects of the contraction are evaluated.

3. Results and discussion

3.1. Loss of lateral force transmission due to the release of fibers

From the analysis of the experimental protocol of Huijing et al. [15], as expected, a drop in the total force is observed when a fiber is released and left free to shorten. However, as in the experimental protocol, this drop (Fig. 5, blue dots) is much lower than the reduction in the region of fixed-end fibers (Fig. 5, red dots). With only one fiber released, a condition corresponding to an area reduction of 14 %, 98 % of the total tension is transmitted, while when four fibers are released, with a reduction of 58 % of the area, 93 % of the total force is still maintained. Interestingly, the drop of the tension estimated by the numerical analysis is in line with what was observed experimentally at muscle level in an animal model for a similar reduction of area, with a drop of tension of approximately 1 % and 8 % for an area reduction of 25 % and 50 %, respectively [15].

The bundle has still the capability to transmit the contraction force of the fiber through the ECM, but this contraction force is reduced because of the shortening of the fiber, according to the force-length function. The distribution of the values assumed by the force-length function in the bundle for the four phases of fiber release is shown in Fig. 6. In fact, the contraction force is proportional to the value of the force-length function and the latter reduces when the fiber length is shortening below its optimal value. The contour in Fig. 6 b shows a decrease in the values of the force-length function, therefore in the corresponding contraction force, with the progressive release of the fibers. In fact, the analysis shows that each fiber release involves a shear deformation of the surrounding ECM (Fig. 6 c), suggesting that the mechanism of lateral transmission of the contraction force is related to the presence of the ECM and its shear stiffness. In other words, the higher the ECM shear deformation, the lower the fiber length with respect to its optimal value and the higher the drop at the same percentage reduction of CSA.

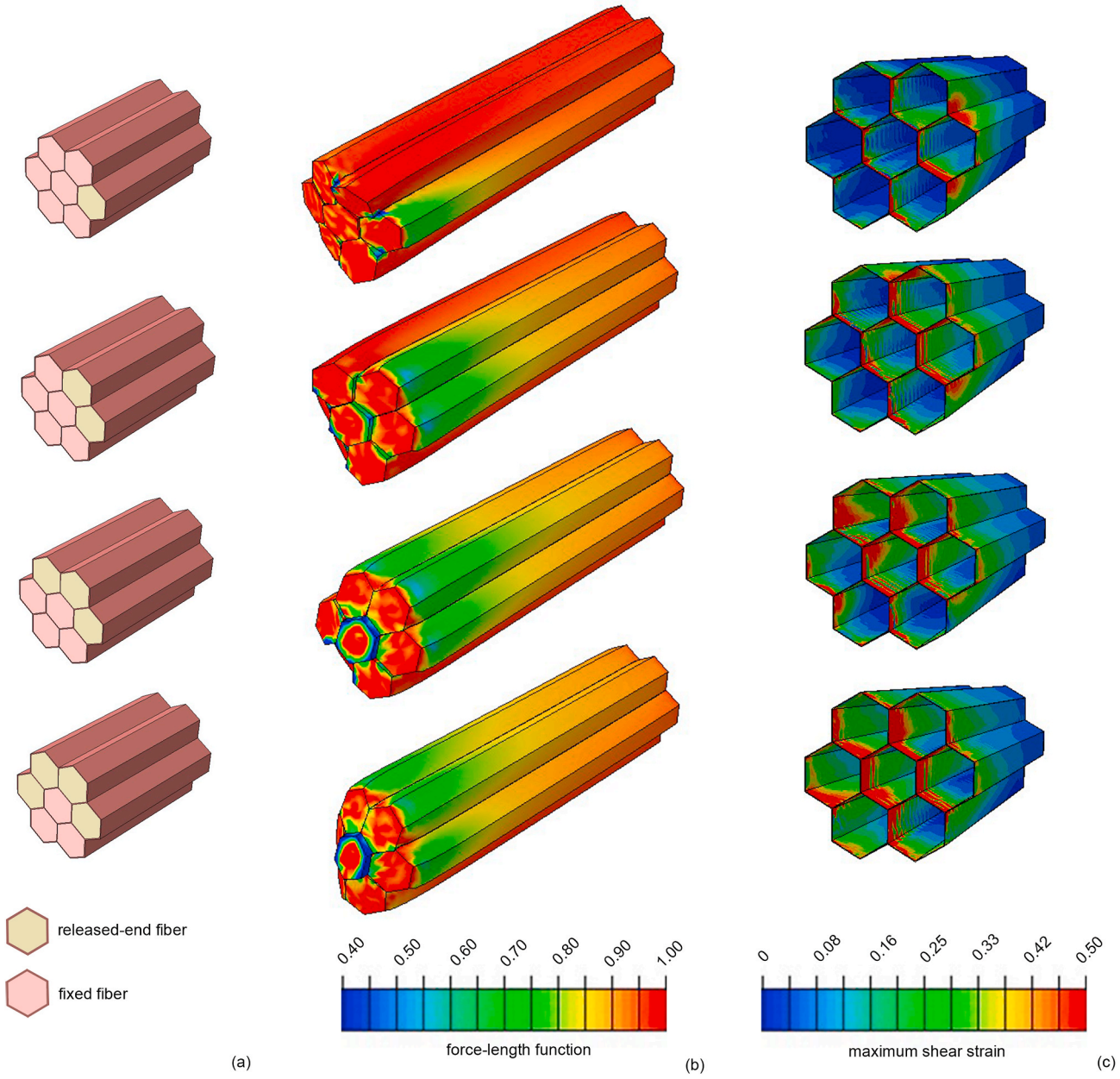

Fig. 6. Schematic representation of fibers release for each of the four phases (a); corresponding force-length distribution (b); maximum shear strain distribution of the ECM (c).

3.2. Effect of age-related increase of ECM thickness on the lateral force transmission

The FEM models of the bundles can be used to estimate the decrease of tension due to the age-related increase in the amount of ECM in the CSA. In fact, as already mentioned, our experimental data on human bundles [38] showed that aging has greater effects on the relative area of the ECM in the bundle than on the intrinsic stiffness of the ECM.

The same numerical analysis performed on the elderly bundle allows comparing the transmitted force loss with that of the young bundle (Fig. 7).

The elderly bundle shows a reduced ability to transmit the contraction force with an increasing number of released fibers. Consequently, at the same percentage loss of CSA, the force reduction in the elderly bundle is greater with respect to the young bundle. Since there are no differences in contractile capability and CSA of the fibers between young and elderly models, the difference in force transmission must be attributed to the configuration of the ECM. This has a lower shear stiffness in the elderly bundle because of its higher thickness. Therefore, the sarcomeres in the elderly bundle work farther from their optimal length and the value of the force-length function is lower, determining also a lower contractile force according to Equation (2). A detailed comparison of the distribution of the force-length function value in young and elderly bundles is shown in Supplementary Fig. S1.

3.3. Lateral and longitudinal force transmission ratio

The comparison of normalized transmitted force between isometric contraction and fiber release under yoke constraint is shown in Fig. 8, for young and elderly bundles. The percentage loss in force transmission for the elderly bundle (−22.2 %) is almost three times higher than the one observed for the young bundle (−7.5 %), due to a lower ability to laterally transmit the contraction force. It is interesting to note that the drops in the numerical analysis for young and elderly bundles are in the

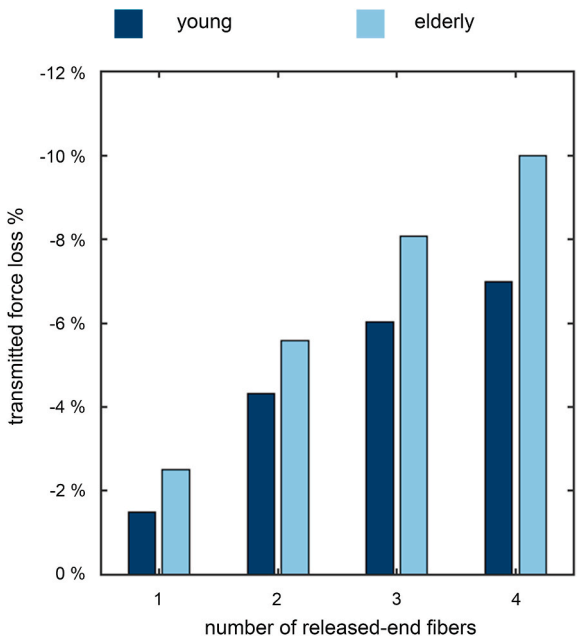

Fig. 7. Comparison of the percentage loss of transmitted force in young and elderly subjects for an increasing number of fibers released.

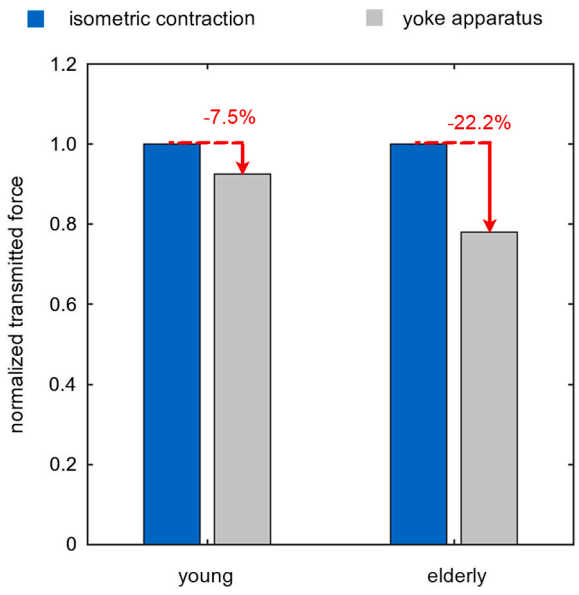

Fig. 8. Normalized transmitted force for young and elderly bundles in the case of isometric contraction and after fiber release with yoke constraint. The percentage loss of transmitted force is shown in red.

order of what was obtained experimentally [14] at the muscle level in an animal model (−20 %, −24 % and −34 % in young, old, and very old rats, respectively).

In this case too, the larger decrease in transmitted force estimated in the elderly bundle can be explained by considering the distribution of the values of the force-length function, reported in Fig. 9 in the middle longitudinal section of the bundles.

After fiber release, the presence of the yoke and the shear stiffness of the ECM limit the shortening of the fibers in the region between the yoke itself and the fixed end of the bundle. Therefore, the central fiber of the bundle and the inner regions of the external fibers experience a small reduction with respect to the optimal length in the sarcomeres. Therefore, the reaction force acting on the yoke when all fibers are released is

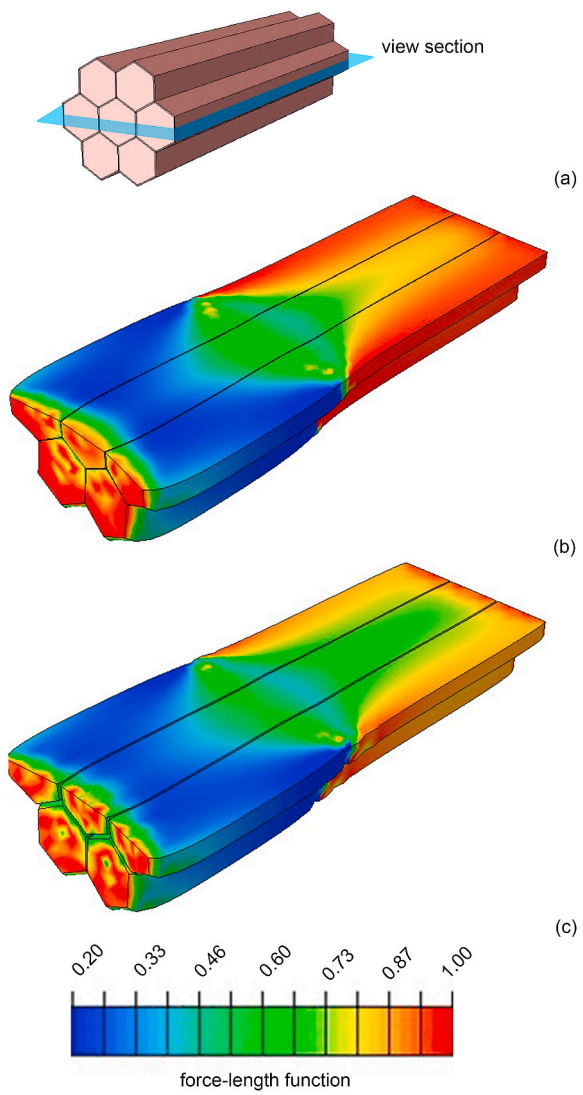

Fig. 9. Middle longitudinal section of the bundle (a); force-length distribution at the maximum contraction for young (b) and elderly (c) bundles after fiber release with yoke constraint.

lower (19.35 mN for young subjects, 16.18 mN for elderly) than the total force generated during isometric contraction (20.92 mN for young subjects, 20.79 mN for elderly), when all fibers are kept at the optimal length. Since the force is transmitted longitudinally in isometric contraction and laterally when the fibers are released, the evaluation of the ratio of forces transmitted under the two conditions can be related to the effects of ECM shear stiffness.

In the region between the yoke and the fixed end of the bundle, the fibers of the young bundle show higher values of the force-length function than those of the elderly bundle, resulting in a greater ability to generate force, according to Equation (2). This is due to the higher thickness of the ECM in the elderly bundle, resulting in a lower shear stiffness and, consequently, in a higher shortening of the fibers.

In summary, the numerical results obtained for young and elderly bundles show that an age-related increase in the thickness of the ECM can explain the reduction in the ECM shear stiffness and, therefore, a reduction in the ability to transmit the contraction force through a lateral transmission mechanism. This is found in the numerical analyses inspired by both the experimental protocols considered in this work.

The proposed approach is based on some assumptions to reduce the complexity of the analyses, but at the same time presents some limitations, which are discussed in the following.

The geometry of the model is simplified with respect to an actual bundle configuration. Indeed, a simplified geometry allows varying the relative amount of ECM in a precise way, without introducing other differences between the young and elderly models and consequently a possible bias. However, this is a reasonable assumption because the bundle shows a certain level of shape regularity in the histological sections (as shown in Fig. 1) and the model geometry is similar to what can be observed.

The increase in the relative amount of ECM from young to elderly bundles is estimated based on experimental data from a previous study [32]. Even if these are limited to a few subjects, they represent an interesting set of experimental data on humans of different ages.

In line with the literature, for example as proposed by Zhang et al. [35], the constitutive modeling of the ECM in this work is carried out assuming an isotropic behavior. According to this, the shear stiffness of the ECM is deduced from tensile tests on the bundles [37]. Although the hypothesis of mechanical anisotropy of the ECM was already proposed in literature [33], an experimental basis is missing to support it. Thus, a reliable constitutive model describing this anisotropy from a quantitative point of view cannot be defined at present.

In this work, the investigation of lateral transmission of force is limited at the level of muscle bundles, which represents the typical size of the samples used in our *ex vivo* experiments [37,38]. An improving development could be targeted to scale up these models to the level of the whole muscle. This would enable to verify if the role of ECM in the lateral transmission of force is confirmed by considering the shear stiffness of perimysium and epimysium.

Despite the limitations presented, we could state that our findings agree with the literature, as a greater force loss is found in elderly subjects. Therefore, the quantitative data obtained by numerical simulations support the idea that the increased thickness of the ECM play a role in the decay of the lateral transmission of force in the elderly with respect to young subjects. This, in turn, may explain the disproportionate loss of muscle force compared to muscle mass in aging, paving the way for future experimental analysis.

4. Conclusion

The aim of the present work is to highlight the possible effect of an age-related increase in ECM thickness on contraction force transmission in human subjects. For this purpose, two numerical models of a muscle bundle have been developed for young and elderly subjects, only with a different thickness of the ECM layer surrounding the fibers. Other age-dependent modifications, such as changes in the intrinsic properties and in the ability to generate contraction force, are not considered to better highlight the main role of the increase in the amount of ECM.

Numerical simulations, inspired by experimental protocols from the literature, are carried out at the scale of a bundle to quantify the transmitted force. Our results show that an increase of the ECM thickness, a condition observed experimentally, is sufficient to cause a reduction of the shear stiffness and, consequently, an impaired ability to transmit the contraction force laterally. In turn, this reduced lateral transmission will cause a reduction in the force exerted by the muscles on the bones, causing an impairment in motor ability.

CRediT authorship contribution statement

Silvia Spadoni: Writing – original draft, Visualization, Software, Investigation, Formal analysis. **Silvia Todros:** Writing – original draft, Methodology, Investigation. **Carlo Reggiani:** Writing – review & editing, Methodology, Conceptualization. **Lorenzo Marcucci:** Writing – review & editing, Supervision, Project administration, Methodology, Conceptualization. **Piero G. Pavan:** Writing – review & editing, Supervision, Project administration, Methodology, Conceptualization.

Declaration of competing interest

None

Acknowledgements

The authors acknowledge the CINECA award under the ISCRA initiative, for the availability of high-performance computing resources and support.

Appendix A. Supplementary data

Supplementary data to this article can be found online at https://doi.org/10.1016/j.compbiomed.2024.108488.

References

[1] T. Rantanen, Muscle strength, disability and mortality, Scand, J. Med. Sci. Sports. 13 (2003) 3–8, https://doi.org/10.1034/j.1600-0838.2003.00298.x.
[2] M. Billot, R. Calvani, A. Urtamo, J.L. Sánchez-Sánchez, C. Ciccolari-Micaldi, M. Chang, R. Roller-Wirnsberger, G. Wirnsberger, A. Sinclair, M.N. Vaquero-Pinto, S. Jyväkorpi, H. Öhman, T. Strandberg, J.M. Schols, A.M. Schols, N. Smeets, E. Topinkova, H. Michalkova, A.R. Bonfigli, F. Lattanzio, L. Rodríguez-Mañas, H. Coelho, M. Broccatelli, M.E. D'Elia, D. Biscotti, E. Marzetti, E. Freiberger, Preserving mobility in older adults with physical frailty and sarcopenia: opportunities, challenges, and recommendations for physical activity interventions, Clin. Interv. Aging 15 (2020) 1675–1690, https://doi.org/10.2147/CIA.S253535.
[3] W.J. Evans, W.W. Campbell, Sarcopenia and age-related changes in body composition and functional capacity, J. Nutr. 123 (1993) 465–468, https://doi.org/10.1093/jn/123.suppl_2.465.
[4] M. Visser, M. Pahor, D.R. Taaffe, B.H. Goodpaster, E.M. Simonsick, A.B. Newman, M. Nevitt, T.B. Harris, Relationship of interleukin-6 and tumor necrosis factor- with muscle mass and muscle strength in elderly men and women: the health ABC study, J. Gerontol. A Biol. Sci. Med. Sci. 57 (2002) M326–M332, https://doi.org/10.1093/gerona/57.5.M326.
[5] T. Rantanen, K. Avlund, H. Suominen, M. Schroll, K. Frändin, E. Pertti, Muscle strength as a predictor of onset of ADL dependence in people aged 75 years, Aging Clin. Exp. Res. 14 (2002) 10–15.
[6] L. Marcucci, C. Reggiani, Increase of resting muscle stiffness, a less considered component of age-related skeletal muscle impairment, Eur. J. Transl. Myol. 30 (2020) 8982, https://doi.org/10.4081/ejtm.2019.8982.
[7] P. Laukkanen, E. Heikkinen, M. Kauppinen, Muscle strength and mobility as predictors of survival in 75–84 Year old people, Age Ageing 24 (1995) 468–473, https://doi.org/10.1093/ageing/24.6.468.
[8] E.J. Metter, L.A. Talbot, M. Schrager, R. Conwit, Skeletal muscle strength as a predictor of all-cause mortality in healthy men, J. Gerontol. A biol, Sci. Med. Sci. 57 (2002) B359–B365, https://doi.org/10.1093/gerona/57.10.B359.
[9] A.B. Newman, V. Kupelian, M. Visser, E.M. Simonsick, B.H. Goodpaster, S. B. Kritchevsky, F.A. Tylavsky, S.M. Rubin, T.B. Harris, Strength, but not muscle mass, is associated with mortality in the health, aging and body composition study cohort, J. Gerontol. A Biol. Sci. Med. Sci. 61 (2006) 72–77, https://doi.org/10.1093/gerona/61.1.72.
[10] T. Rantanen, T. Harris, S.G. Leveille, M. Visser, D. Foley, K. Masaki, J.M. Guralnik, Muscle strength and body mass index as long-term predictors of mortality in initially healthy men, J. Gerontol. A Biol. Sci. Med. Sci. 55 (2000) M168–M173, https://doi.org/10.1093/gerona/55.3.M168.
[11] B.H. Goodpaster, S.W. Park, T.B. Harris, S.B. Kritchevsky, M. Nevitt, A.V. Schwartz, E.M. Simonsick, F.A. Tylavsky, M. Visser, A.B. Newman, The loss of skeletal muscle strength, mass, and quality in older adults: the health, aging and body composition study, J. Gerontol. A Biol. Sci. Med. Sci. 61 (2006) 1059–1064, https://doi.org/10.1093/gerona/61.10.1059.
[12] M.V. Narici, C.N. Maganaris, Adaptability of elderly human muscles and tendons to increased loading, J. Anat. 208 (2006) 433–443, https://doi.org/10.1111/j.1469-7580.2006.00548.x.
[13] S.F. Street, Lateral transmission of tension in frog myofibers: a myofibrillar network and transverse cytoskeletal connections are possible transmitters, J. Cell. Physiol. 114 (1983) 346–364, https://doi.org/10.1002/jcp.1041140314.
[14] K.S. Ramaswamy, M.L. Palmer, J.H. van der Meulen, A. Renoux, T. Y. Kostrominova, D.E. Michele, J.A. Faulkner, Lateral transmission of force is impaired in skeletal muscles of dystrophic mice and very old rats, J. Physiol. 589 (2011) 1195–1208, https://doi.org/10.1113/jphysiol.2010.201921.
[15] P.A. Huijing, G.C. Baan, G.T. Rebel, Non-myotendinous force transmission in rat extensor digitorum longus muscle, J. Exp. Biol. 201 (1998) 683–691, https://doi.org/10.1242/jeb.201.5.683.
[16] K. Minato, Y. Yoshimoto, T. Kurosawa, K. Watanabe, H. Kawashima, M. Ikemoto-Uezumi, A. Uezumi, Measurement of lateral transmission of force in the extensor digitorum longus muscle of young and old mice, Int. J. Mol. Sci. 22 (2021) 12356, https://doi.org/10.3390/ijms222212356.
[17] L.K. Wood, E. Kayupov, J.P. Gumucio, C.L. Mendias, D.R. Claflin, S.V. Brooks, Intrinsic stiffness of extracellular matrix increases with age in skeletal muscles of

mice, J. Appl. Physiol. 117 (2014) 363–369, https://doi.org/10.1152/japplphysiol.00256.2014.
[18] A.R. Gillies, R.L. Lieber, Structure and function of the skeletal muscle extracellular matrix, Muscle Nerve 44 (2011) 318–331, https://doi.org/10.1002/mus.22094.
[19] T.W. Kragstrup, M. Kjaer, A.L. Mackey, Structural, biochemical, cellular, and functional changes in skeletal muscle extracellular matrix with aging, Scand. J. Med. Sci. Sports 21 (2011) 749–757, https://doi.org/10.1111/j.1600-0838.2011.01377.x.
[20] A. Bailey, Molecular mechanisms of ageing in connective tissues, Mech. Ageing Dev. 122 (2001) 735–755, https://doi.org/10.1016/S0047-6374(01)00225-1.
[21] M. Boujelbene, A. Majeed, N. Baazaoui, K. Barghout, N. Ijaz, N. Abu-Libdeh, S. Naeem, I. Khan, M.R. Ali, Effect of electrostatic force and thermal radiation of viscoelastic nanofluid flow with motile microorganisms surrounded by PST and PHF: Bacillus anthracis in biological applications, Case Stud. Therm. Eng. 52 (2023) 103691, https://doi.org/10.1016/j.csite.2023.103691.
[22] P. Barnoon, F. Bakhshandehfard, Thermal management in a biological tissue in order to destroy tissue under local heating process, Case Stud. Therm. Eng. 26 (2021) 101105, https://doi.org/10.1016/j.csite.2021.101105.
[23] H. Waqas, U. Farooq, A. Hassan, D. Liu, S. Noreen, R. Makki, M. Imran, M.R. Ali, Numerical and Computational simulation of blood flow on hybrid nanofluid with heat transfer through a stenotic artery: silver and gold nanoparticles, Results Phys. 44 (2023) 106152, https://doi.org/10.1016/j.rinp.2022.106152.
[24] P. Barnoon, M. Ashkiyan, Magnetic field generation due to the microwaves by an antenna connected to a power supply to destroy damaged tissue in the liver considering heat control, J. Magn. Mater. 513 (2020) 167245, https://doi.org/10.1016/j.jmmm.2020.167245.
[25] B. Maayah, A. Moussaoui, S. Bushnaq, O. Abu Arqub, The multistep Laplace optimized decomposition method for solving fractional-order coronavirus disease model (COVID-19) via the Caputo fractional approach, Demonstr. Math. 55 (2022) 963–977, https://doi.org/10.1515/dema-2022-0183.
[26] B. Maayah, O. Abu Arqub, S. Alnabulsi, H. Alsulami, Numerical solutions and geometric attractors of a fractional model of the cancer-immune based on the Atangana-Baleanu-Caputo derivative and the reproducing kernel scheme, Chin. J. Phys. 80 (2022) 463–483, https://doi.org/10.1016/j.cjph.2022.10.002.
[27] P. Pavan, E. Monti, M. Bondí, C. Fan, C. Stecco, M. Narici, C. Reggiani, L. Marcucci, Alterations of extracellular matrix mechanical properties contribute to age-related functional impairment of human skeletal muscles, Int. J. Mol. Sci. 21 (2020) 3992, https://doi.org/10.3390/ijms21113992.
[28] C.A. Yucesoy, B.H.F.J.M. Koopman, P.A. Huijing, H.J. Grootenboer, Three-dimensional finite element modeling of skeletal muscle using a two-domain approach: linked fiber-matrix mesh model, J. Biomech. 35 (2002) 1253–1262, https://doi.org/10.1016/S0021-9290(02)00069-6.
[29] C.A. Yucesoy, B.H.F.J.M. Koopman, G.C. Baan, H.J. Grootenboer, P.A. Huijing, Effects of inter- and extramuscular myofascial force transmission on adjacent synergistic muscles: assessment by experiments and finite-element modeling, J. Biomech. 36 (2003) 1797–1811, https://doi.org/10.1016/S0021-9290(03)00230-6.
[30] C. Zhang, Y. Gao, Finite element analysis of mechanics of lateral transmission of force in single muscle fiber, J. Biomech. 45 (2012) 2001–2006, https://doi.org/10.1016/j.jbiomech.2012.04.026.
[31] C. Zhang, Y. Gao, The role of transmembrane proteins on force transmission in skeletal muscle, J. Biomech. 47 (2014) 3232–3236, https://doi.org/10.1016/j.jbiomech.2014.07.014.
[32] J.A. Hodgson, S.-W. Chi, J.P. Yang, J.-S. Chen, V.R. Edgerton, S. Sinha, Finite element modeling of passive material influence on the deformation and force output of skeletal muscle, J. Mech. Behav. Biomed. Mater. 9 (2012) 163–183, https://doi.org/10.1016/j.jmbbm.2012.01.010.
[33] B. Sharafi, S.S. Blemker, A micromechanical model of skeletal muscle to explore the effects of fiber and fascicle geometry, J. Biomech. 43 (2010) 3207–3213, https://doi.org/10.1016/j.jbiomech.2010.07.020.
[34] K.M. Virgilio, K.S. Martin, S.M. Peirce, S.S. Blemker, Multiscale models of skeletal muscle reveal the complex effects of muscular dystrophy on tissue mechanics and damage susceptibility, Interface Focus 5 (2015) 20140080, https://doi.org/10.1098/rsfs.2014.0080.
[35] Y. Zhang, J. Chen, Q. He, X. He, R.R. Basava, J. Hodgson, U. Sinha, S. Sinha, Microstructural analysis of skeletal muscle force generation during aging, Int. J. Numer. Method Biomed. Eng. 36 (2020), https://doi.org/10.1002/cnm.3295.
[36] B. Sharafi, S.S. Blemker, A mathematical model of force transmission from intrafascicularly terminating muscle fibers, J. Biomech. 44 (2011) 2031–2039, https://doi.org/10.1016/j.jbiomech.2011.04.038.
[37] L. Marcucci, C. Reggiani, A.N. Natali, P.G. Pavan, From single muscle fiber to whole muscle mechanics: a finite element model of a muscle bundle with fast and slow fibers, Biomech. Model. Mechanobiol. 16 (2017) 1833–1843, https://doi.org/10.1007/s10237-017-0922-6.
[38] L. Marcucci, M. Bondì, G. Randazzo, C. Reggiani, A.N. Natali, P.G. Pavan, Fibre and extracellular matrix contributions to passive forces in human skeletal muscles: an experimental based constitutive law for numerical modelling of the passive element in the classical Hill-type three element model, PLoS One 14 (2019) e0224232, https://doi.org/10.1371/journal.pone.0224232.
[39] S. Todros, N. de Cesare, G. Concheri, A.N. Natali, P.G. Pavan, Numerical modelling of abdominal wall mechanics: the role of muscular contraction and intra-abdominal pressure, J. Mech. Behav. Biomed. Mater. 103 (2020) 103578, https://doi.org/10.1016/j.jmbbm.2019.103578.
[40] S. Todros, N. de Cesare, S. Pianigiani, G. Concheri, G. Savio, A.N. Natali, P. G. Pavan, 3D surface imaging of abdominal wall muscular contraction, Comput. Methods Progr. Biomed. 175 (2019) 103–109, https://doi.org/10.1016/j.cmpb.2019.04.013.
[41] N. de Cesare, C. Trevisan, E. Maghin, M. Piccoli, P.G. Pavan, A finite element analysis of diaphragmatic hernia repair on an animal model, J. Mech. Behav. Biomed. Mater. 86 (2018) 33–42, https://doi.org/10.1016/j.jmbbm.2018.06.005.
[42] S.K. Gollapudi, D.C. Lin, Experimental determination of sarcomere force–length relationship in type-I human skeletal muscle fibers, J. Biomech. 42 (2009) 2011–2016, https://doi.org/10.1016/j.jbiomech.2009.06.013.